J. Korean Inst. Electr. Electron. Mater. Eng.
Vol. 36, No. 1, pp. 1-9 January 2023
DOI: https://doi.org/10.4313/JKEM.2023.36.1.1
ISSN 1226-7945(Print), 2288-3258(Online)

Academic Progress Report

Study on Solution-Processed Flexible Electrochromic Devices with Improved Coloration Efficiency and Stability

Gihwan Song and Haekyoung Kim

Institute of Materials Technology, School of Materials Science and Engineering,
Yeungnam University, Gyeongsan 38541, Korea

(Received October 17, 2022; Revised October 31, 2022; Accepted October 31, 2022)

Abstract: According to the recent global warming, it is necessary to use energy efficiently together with eco-friendly energy. The development of alternative technologies is requisite for managing the current energy and climate crises. In this regard, "smart windows," which can control solar radiation, can be used to mitigate energy demands. Electrochromic devices (ECDs) effectively control the amount of solar energy reaching commercial and other living areas and maintain climate conditions via color modulation in response to small external stimuli, such as temperature and light irradiation. However, the performance and the stability of ECDs depend on the state of the electrolyte and sealing of the device. To resolve the aforementioned issues, an ECD was manufactured by using a poly (methyl methacrylate) (PMMA)-based gel polymer electrolyte (GPE), and a laminating method was used to adequately seal the ECD. The concentrations of PMMA, acetonitrile (ACN), and ferrocene (Fc) were controlled to optimize the composition of the GPE to achieve an enhanced electrochromic performance. The fabricated GPE-based ECD afforded high optical contrast (~81.92%), with high electrochromic stability up to 10,000 cycles. Moreover, the lamination method employing the GPE could be used to fabricate large-area ECDs.

Keywords: Electrochromic device, Gel polymer electrolyte, Flexible, Stability, Large-area device

1. INTRODUCTION

Owing to the global energy crisis, the requirement for "smart windows", which can save energy through the chromism phenomenon exhibited by materials, is rapidly increasing [1,2]. Chromism, in which the optical properties of a material can be controlled in response to a stimulus, is divided into passive and active types based on the specific stimulus applied. Such stimuli include electricity (electrochromism), heat (thermochromism), stress (mechanochromism), and light irradiation (photochromism) [3-5]. ECDs are a promising research field in the smart window industry because of their ability to control the amount of incident solar radiation reaching an area through changes in their transmittance [6]. Furthermore, ECDs can be used not only glass, energy storage device, automobile, and organic light emitting diode fields, but also in more fields through flexible substrates such as e-skin and curved architecture [7-11].

In general, the ECDs comprises the EC material, an electrolyte, and an ion conductor between two TCEs in the solid state. Tungsten trioxide (WO_3) is the most attractive EC material with the advantages of a high coloration efficiency and long cyclic stability compared with other transition metal oxides [12]. The electrolyte facilitates ion transfer and can be classified into liquid, solid, or gel types. Liquid-type electrolytes

✉ **Haekyoung Kim; hkkim@ynu.ac.kr**

have been widely used owing to their excellent ion conductivity; however, they possess a few disadvantages, such as low stability due to leakage and vulnerability to heat. Therefore, gel polymer electrolytes (GPEs) have been used to replace liquid electrolytes. In GPEs, a Li salt is added to a polymer matrix, or a GPE, wherein a plasticizer and a solvent are mixed in a polymer matrix. GPEs are known to exhibit good ionic conductivity, thermal stability, electrochemical stability, flexibility, and good contact with the electrodes, and they can be applied to large-area devices [13-16]. Owing to these advantages and recent trends, PEO, PVB, and PVdF-HFP-based GPEs have been used in ECD applications [17-19]. Because these GPEs are extremely useful for application in flexible substrates, they are being actively studied in the field of flexible electronics [20,21]. PMMA is one of the most promising materials as a polymer matrix for GPEs owing to its good mechanical properties, high transmittance, good compatibility with liquid electrolytes, and excellent environmental stability [13]. However, when only the GPE is used, it is difficult to achieve structural simplification as an ion storage layer is required for the ECD. To overcome this problem, herein, Fc was dissolved in a PMMA-based GPE as a redox mediator. Because Fc can be used as an oxidizing material, the electrochromic performance could be improved at a relatively low voltage, which simplified the manufacturing process [22].

In this study, an ECD was fabricated via simple bonding by applying pressure, which is a laminating method that can be easily applied to large-area devices. Thus, it was expected that the ECD fabricated with the PMMA-based GPE could be easily accessed as a roll-to-roll system and could be widely used commercially. Herein, GPEs were synthesized by varying the concentration of PMMA and Fc, and an optimized ECD was fabricated by controlling the hardening time before lamination. The optimized ECD was found to exhibit a high transmittance change (ΔT) of 81.92% at a relatively low voltage (−1.25 V). The ECD also demonstrated an excellent stability while maintaining the transmittance for 10,000 cycles, with only a 4.6% degradation relative to the initial value. Moreover, a large-area device was fabricated using the lamination method.

2. EXPERIMENTAL

2.1 Materials

PMMA (average M_w ~350,000, Sigma-Aldrich), PC (anhydrous, 99.7%, Sigma-Aldrich), ACN (Duksan, South Korea), lithium perchlorate ($LiClO_4$, 99%, Acros Organics), and Fc (Sigma-Aldrich) were used to synthesize the PMMA-based GPEs. ITO-coated PET substrates (R_{sh} = 30 Ω/square, Hansung Industry Corporation, South Korea) were used as conducting substrates. Tungsten powder (APS 1–5 μm, 99.9%, metals basis, Alfa Aesar) and hydrogen peroxide (Duksan, South Korea) were used to synthesize the tungsten trioxide (WO_3) powder.

2.2 Preparation of the PMMA gel polymer electrolyte

To prepare the PMMA-based GPEs, $LiClO_4$ (3 wt%) was dissolved in a mixture of ACN (63.4, 66.4, and 69.4 wt%) and PC (20 wt%). Thereafter, PMMA powder (7, 10, and 13 wt%) was added slowly to the prepared solution, and the solution was stirred overnight at room temperature. Finally, Fc powder (0.6 wt%) was added as an anodic species and oxidizing agent to synthesize the PMMA-based GPEs.

2.3 Synthesis of WO_3

WO_3 was synthesized as described in our previous report [23]. First, tungsten powder (6.8 g) and H_2O_2 (93.2 g, 31 wt% in H_2O) were blended and stirred for 2 h. The blended solution was heated to 100°C to evaporate the solvent, after which the pale yellow WO_3 powder was obtained.

2.4 Fabrication of ECD

First, WO_3 powder (30 wt%) was dispersed in a DI water/isopropanol (1/1 wt%) mixture by ultrasonication for 6 h. A thin film of WO_3 was coated on the ITO/PET substrate using thespin-coating method (speed = 5000 rpm, time = 25 s). The fabricated WO_3 thin film on ITO was annealed at 60°C for 8 h in a vacuum oven [24]. Thereafter, the PMMA-based GPE (0.45 g) was dropped cast on the WO_3 thin film kept in an oven at 80°C to remove the solvent (hardening process). The

hardening process was performed for different time intervals (3, 4, and 5 min). Subsequently, another ITO/PET substrate was placed on top of the assembly, which was laminated at room temperature to obtain flexible ECDs with a PMMA-based GPE.

2.5 Characterization

To study the ionic conductivity of the PMMA-based GPE, GPEs were prepared by varying the PMMA concentration, without Fc, and were assembled between two ITO/PET electrodes using the lamination method after hardening the GPEs (4 min) [25]. The electrochromic performance was measured using an electrochemical workstation (ZIVE SP10, WonaATech, South Korea) and an ultraviolet–visible spectrometer (Thermo Scientific, South Korea). The morphology of the fabricated ECDs was observed by SEM. Prior to the data analysis, the electrochromic response of all samples was measured after 500 repetitions of testing to ensure that the electrolyte penetrated both the electrodes well. The electrochromic performance was analyzed as a function of time, and the coloration and bleaching processes were performed in the range of –1.25 to 0 V, with excitation at 700 nm; the coloring and bleaching processes were performed for 2 min each. For rectangular device structures, coloring and bleaching were respectively performed for 4 min to observe the electrochromic saturation.

3. RESULTS AND DISCUSSION

The ionic conductivity and viscosity are essential parameters that influence the electrochemical reaction and fabrication of the GPE system. The ionic conductivity was calculated using Eq. (1):

$$\sigma = d / (R \times A) \quad (1)$$

where R is the resistance of the GPE, which was measured via the EIS analysis. Here, A is the active area of the ECD, and *d* is the distance of the two electrodes after bonding, which varies with the PMMA concentration; d (μm) was measured using a thickness meter. A exhibited a constant value (6.25 cm^2), whereas d increased with an increase in the polymer concentration, which influenced the features of the assembled device; thus, the d values were ~75.2, ~121, and ~154 μm when the PMMA concentration was 7, 10, and 13 wt%, respectively. The ionic conductivity ($S \cdot cm^{-1}$) was calculated to be 3.98×10^{-5}, 6.81×10^{-5}, and 8.13×10^{-5} at PMMA concentrations of 7, 10, and 13 wt%, respectively. The ionic conductivity increased as the polymer concentration increased because a larger polymer matrix could create additional Li ion pathways to access the electrode. On the other hand, other research groups have reported that such an increase in the ionic conductivity of the GPE occurs because a high PMMA concentration results in a decrease in the crystallinity and an increase in the amorphous nature of the GPE, facilitating the creation of free ions. [26-28]. The viscosity which defines resistance of a fluid to a change in shape or movement was found to be 30, 310, and 2,450 cP when the PMMA concentration was 7, 10, and 13 wt%, respectively. The viscosity increased significantly as the PMMA concentration increased.

To study the effect of the hardening time on the electrochromic performance of ECDs, a GPE with 10 wt%

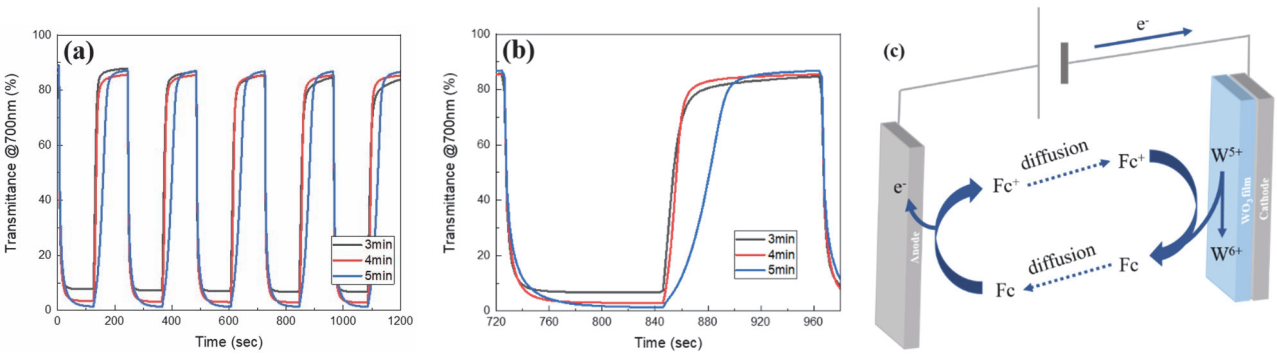

Fig. 1. Electrochromic performance according to hardening time. (a) 5 cycles, (b) 1cycle, and (c) self-bleaching mechanism of Fc.

PMMA and 0.6 wt% Fc was employed in the ECD. Figure 1 ((a) and (b)) illustrates the electrochromic performance achieved with the PMMA-based GPE under different hardening conditions. Here, ΔT is the calculated average difference between the transmittance of the saturated regime for the bleached and colored states of the device. The value of ΔT is 77.94, 81.92, and 83.96%, and the GPE thickness is ~64.8, ~97.8, and ~114.8 μm for hardening times of 3, 4, and 5 min, respectively. Thus, the thickness and ΔT were found to increase with longer hardening periods. Because a longer hardening time can result in more facile bonding of the polymer chains to the electrodes, the thickness increased with a longer hardening time. A high thickness indicates that additional Li ions exist in the device; thus, ΔT also increased with increasing hardening time.

The switching time was calculated from the moment the voltage was changed until ΔT reached 90%. The switching time increased with the hardening time because of the high polymer content. In particular, the bleaching time dramatically increased from 17s to 47s. To explain this phenomenon, a possible mechanism underlying the device operation was proposed (Fig. 1(c)). In the colored state, Fc is oxidized near the anode and diffuses to the cathode owing to its easy oxidation. However, the reduction potential of Fc^+/Fc is higher than that of the WO_3 film; hence, it only acts as an oxidizing agent [22]. However, as the thickness of the GPE increases, the diffusion of Fc^+ is hindered by the PMMA matrix; thus, the ratio of Fc^+ that diffuses to WO_3 will decrease, and the bleaching time will be relatively slow. For the sample prepared with a hardening time of 3 min, the optical contrast and bleaching time were lower than those for the sample with a hardening time of 4 min owing to the short hardening time required for bonding with both electrodes in the former case. Therefore, the optical contrast was relatively good for the latter, and a fast switching time was required for the same; therefore, a hardening time of 4 min was selected for further experiments.

To study the effect of the Fc concentration on the electrochromic performance of the ECD, the GPE prepared with 10 wt% PMMA, and a hardening time of 4 min was selected. Fig. 2((a) and (b)) depicts the electrochromic response of the ECDs with different Fc concentrations (0.2, 0.6, 1.0 wt%). Here, the value of ΔT is 35.66, 81.92, and 74.99%, and the bleaching time is 35, 17, and 17 s with respective Fc concentrations of 0.2, 0.6, and 1.0 wt%. The GPE thickness and coloring time were similar irrespective of the Fc concentration (Fig. 2(a) and (b)). Thus, it was confirmed that the optical contrast and bleaching time increased at Fc concentrations of 0.6 and 1.0 wt%. This can be ascribed to the reduction of WO_3, which indicates that the bleaching process was inefficient owing to the lack of Fc^+ as an anodic species, although WO_3 was sufficiently reduced (colored) during the cycle before the performance analysis. However, with 1.0 wt% Fc, the optical performance of the device degraded because, as depicted in the SEM image (Fig. 3), agglomeration of Fc hinders the movement of the ions. This agglomeration also reduces the preferred orientation in the bleached state. Therefore, the ECD performance was optimized at a concentration of 0.6 wt% Fc.

The effect of the PMMA concentration on the electrochromic performance of the device is illustrated in Fig. 4. The sample was prepared with a hardening time of 4 min and a concentration of 0.6 wt% Fc, which were the optimal conditions, as determined above. The value of ΔT was 64.73, 81.92, and 81.78%, and the

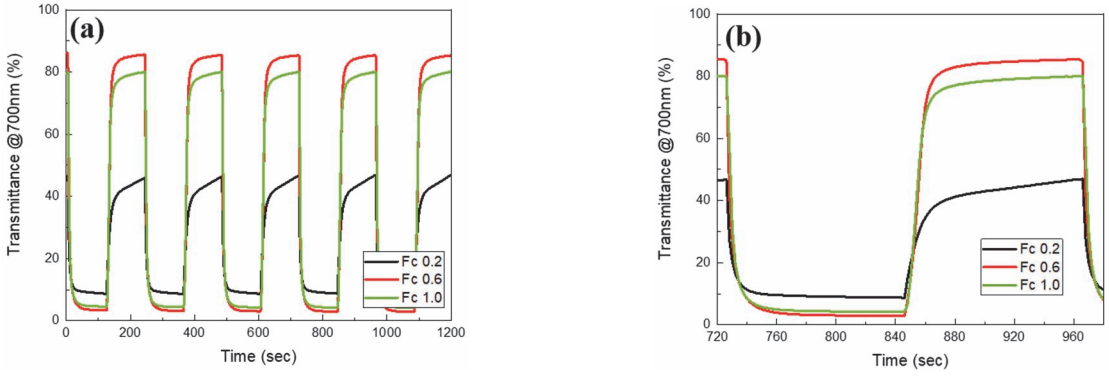

Fig. 2. Electrochromic performance according to Fc concentration. (a) 5 cycles and (b) 1 cycle.

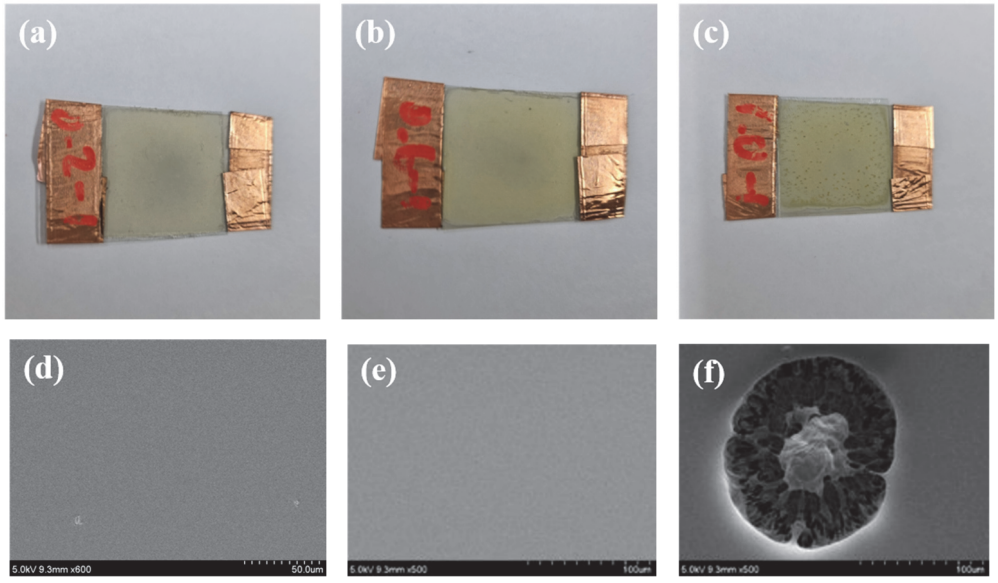

Fig. 3. Photo image of (a) Fc 0.2 wt%, (b) Fc 0.6 wt%, (c) Fc 1.0wt%, SEM image of (d) Fc 0.2 wt%, (e) Fc 0.6 wt%, and (f) Fc 1.0 wt%.

bleaching time was 9, 17, and 21 s at respective PMMA concentrations of 7, 10, and 13 wt%. The coloring time was similar irrespective of the PMMA concentration; the GPE thickness was ~66.8, ~97.8, and ~127.8 μm at PMMA concentrations of 7, 10, and 13 wt%, respectively (Fig. 4(a) and (b)). It was confirmed that adding 7 wt% PMMA led to a lower ΔT than that obtained with 10 wt% and 13 wt% PMMA owing to the low polymer concentration and ionic conductivity of PMMA. For the ECD employing 13 wt% PMMA, ΔT was approximately similar to that of the ECD employing 10 wt% PMMA; however, the former exhibited a relatively slow bleaching time, which probably resulted in a greater thickness of the GPE with an increasing PMMA concentration. As the PMMA concentration increased, the thickness of the GPE increased, which may be attributed to the diffusion mechanism of Fc^+ described above. Figure 4(c) displays the coloration efficiency (CE) with respect to the PMMA concentration. The CE is an important performance indicator for ECDs. The CE represents the optical density per injected charge density and is the transmittance change that can be induced by a specific current. Equation (2) expresses the CE, as follows:

$$\mathrm{CE}(\eta) = \Delta OD/\Delta Q = \log(T_b/T_c)/\Delta Q \quad (2)$$

where ΔOD is the change in the optical density, ΔQ is the amount of injected charge corresponding to ΔOD, and T_b and T_c are the transmittance values under the bleached and colored conditions, respectively. Using this equation, the CE at −1.25 V was extracted from the slope in the linear regime. The CE

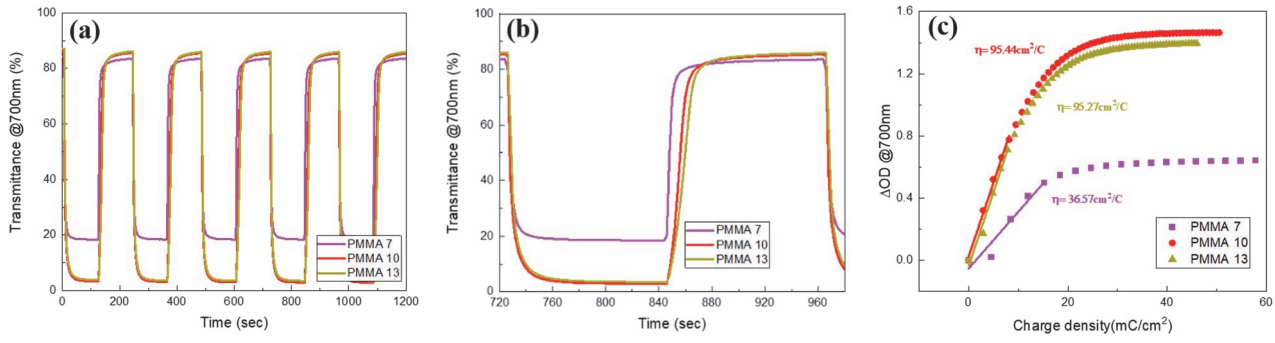

Fig. 4. Electrochromic performance according to PMMA concentration (a) 5 cycles, (b) 1 cycle, and (c) coloration efficiency.

values of the optimized ECD were 36.57, 95.44, and 95.27 cm^2/C with 7, 10, and 13 wt% PMMA, respectively. The devices with 10 and 13 wt% PMMA exhibited a higher CE than the device with 7 wt% PMMA owing to the better adhesion of the GPE to the electrode and high ionic conductivity in the former case. The highest CE value (95.44 cm^2/C) of the device with 10 wt% PMMA is better than or comparable to that reported in a previous study based on the electrochromic performance of an ECD with a GPE [20,38]. The high CE value reveals that a relatively low current can result in a high optical contrast, and the ECD can save energy more efficiently.

Therefore, the ECD fabricated with the PMMA-based GPE was found to be optimized when 0.6 wt% Fc, 10 wt% or 13 wt% PMMA, and a hardening time of 4 min were used for the GPE. However, the GPE with 13 wt% PMMA was difficult to handle owing to its very high viscosity and slow bleaching time. Hence, the optimal concentration of 10 wt% PMMA was used to achieve a relatively low viscosity, high CE, fast bleaching time, and uniform bonding to large-area substrates.

The performance of this optimized ECD is plotted versus the wavelength and voltage (Fig. 5(a) and (b)). At 757 nm, ΔT reaches a maximum of 85% (Fig. 5(a)), and even at 550 nm, where the human eye is sensitive, the optical contrast is relatively good (72%). Figure 5(b) illustrates the gradation characteristics according to the voltage. Based on these observations, we can conclude that the optimized device demonstrates potential for use in various fields such as sensors, displays, and smart windows. Figure 5(c) presents a stability test in which the laminated ECD, with the PMMA-based GPE, was subjected to 10,000 electrochromic cycles. The stability test was conducted by applying 0 V to −1.25 V during each coloring and bleaching cycle for 10 s and then measuring ΔT by applying a switching time of 2 min at −1.25 V, every 1,000 cycles. Equation (3) was used to determine the degradation value.

$$\text{Degradation (\%)} = \{(\Delta T_{initial} - \Delta T_{final}) / \Delta T_{initial}\} \times 100 \quad (3)$$

The percentage degradation of the laminated ECD, employing the PMMA-based GPE, was 4.6%. A stable performance was obtained without electrolyte leakage by densely bonding the gel polymer electrolyte via the lamination method.

The electrochromic performance of an ECD with a spacious rectangular structure was studied for more detailed applications. The first type of device had a vertically long structure (2.5 cm × 7.5 cm), and the other had a horizontally long structure (7.5 cm × 2.5 cm). Figure 6(a) depicts the electrochromic performance of the rectangular ECDs. It was confirmed that the optical contrast (~82.74%) and coloring time (~9 s) achieved with the vertically long device were similar to those of the small device (2.5 cm × 2.5 cm). However, the horizontally long device exhibited a low transmittance (~63.64%) and low coloring time (~35 s) as the electrons might not have been sufficiently transferred to reduce the WO_3 film. Thus, it was revealed that a specific structure facilitating electron transfer could influence the electrochromic performance. Therefore, we believe that if the electron transfer can be controlled through a flexible configuration, various creative applications will be possible.

Furthermore, bending tests were conducted to study the electrochromic response over several bending cycles at a bending radius (r) of 0.5 cm and 1 cm, respectively. Figure

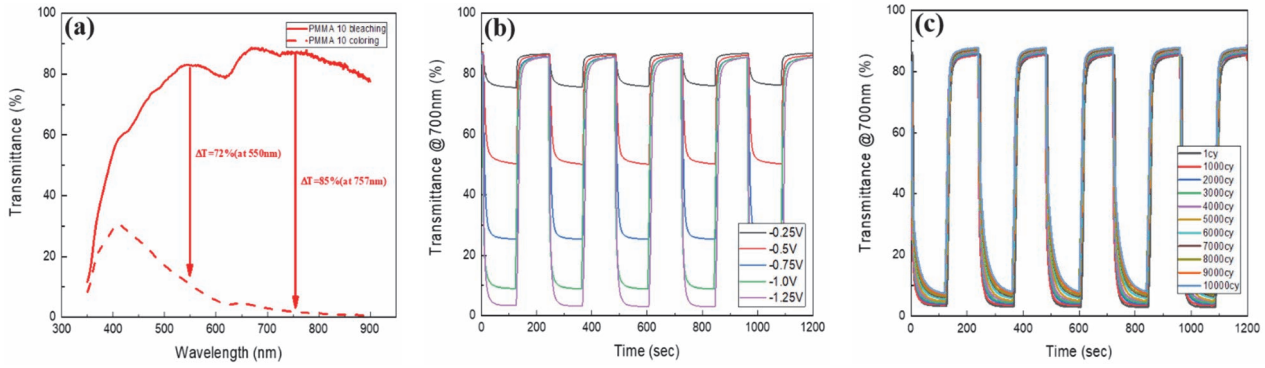

Fig. 5. Optimized ECD performance with (a) wavelength, (b) voltage, and (c) stability for 10,000 cycles.

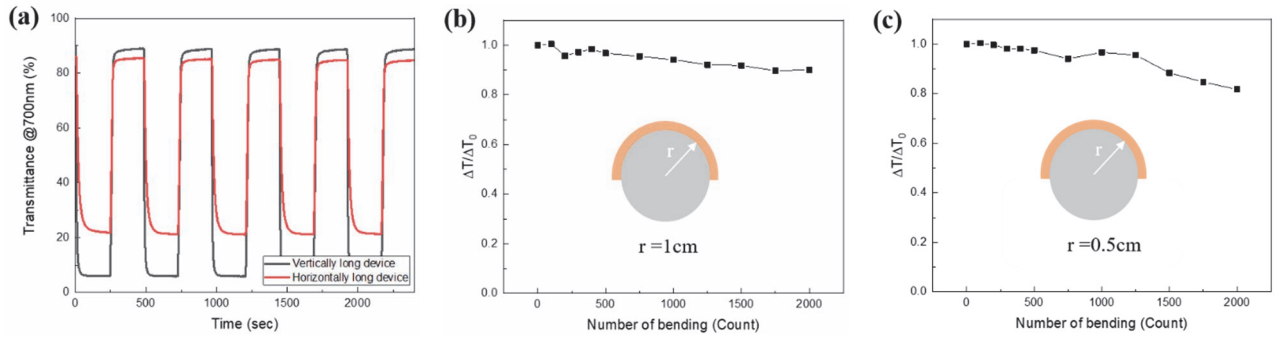

Fig. 6. (a) Rectangular ECD performance and bending cycles with different bending radius (b) 1 cm, and (c) 0.5 cm.

6((b) and (c)) illustrates the observed rate of the transmittance change according to the number of bending cycles. At a high value of *r*, the initial optical contrast of the ECDs is well maintained (~90% after 2,000 bending cycles). Although the degradation is more severe at a lower *r*, it can be confirmed that the electrochromic response is maintained, and the optical contrast remains at ~82% compared with the initial value. It is postulated that this deterioration originates from the decreased conductivity of the ITO electrodes, which are brittle. Thus, a bending test was conducted, and it was confirmed that the resistance of the ITO electrodes increased slightly with the number of bending cycles. Despite the degradation of ITO, the stability over repeated bending cycles was high and comparable to that in previous reports (Table 1). The ability of the device to retain its coloring characteristics, even in the bending state, indicates an extremely high potential for future flexible electro-opto applications.

The obtained results were compared with those of previous studies [20,29-31] based on the ionic conductivity and electrochromic performance of GPE-based ECDs (Table 2). It was confirmed that the ionic conductivity of the ECD employing the PMMA-based GPE with Fc was comparable to that of prior devices, and the transmittance change was comparatively excellent, with a fast switching time. Furthermore, the electrochromic performance and stability were compared with those of previously reported flexible ECDs [32-37] (Table 1). The optimized ECD developed herein not only demonstrated a good electrochromic response but also exhibited a highly stable performance owing to the dense bonding achieved via the lamination method. A large-

Table 1. Electrochromic performance on the flexible substrates.

ECD system	ΔT (%)	$\Delta t_c/\Delta t_b$ (sec)	Stability	Bending test	Ref.
PET/ITO/WO_3-Au/PEDOT/Pt/ PMMA based gel polymer /ITO/PET	26 (750 nm)	19.25/13.83	No test	No test	32
PET/AgNW/PEDOT:PSS/ Viologen based ion gel electrolyte/ PEDOT:PSS/AgNW/ PET	71.9 (604 nm)	13/18	5% loss after 50 cycles	~90% after 20 cycles	33
PET/W/Ag NFs/W/ PVA based gel polymer electrolyte /NiO/Ag NFs/PET	~90 (633 nm)	9/19	13% loss after 300 cycles	~30% after 200 cycles	34
PET/ITO/PEDOT:PSS/ PCL/SiO_2/ITO/PET	30.6 (650 nm)	25.2/17.1	100 cycles	100 cycles	35
ISHCP[a]/ Poly(acrylamide) based hydrogel electrolyte /ISHCP	47.7 (590 nm)	3.3/20.1	10% loss after 1,000 cycles	1,000 cycles	36
PET/ITO/WO_3-PEDOT/ PMMA based gel polymer electrolyte/V_2O_5/ITO/PET	61.5 (750 nm)	13.58/8.07	No test	No test	37
PET/ITO/WO_3/ PMMA based gel polymer electrolyte /ITO/PET	81.92 (700 nm)	9/17	4.6% loss after 10,000 cycles	~90% and ~82% after 2,000 cycles	This work

a. ISHCP: Intrinsically stretchable and highly conductive polymers

Table 2. Ionic conductivity and electrochromic performance of GPE based ECD.

ECD construction	Ionic conductivity (S/cm)	ΔT (%)	Switching time, $\Delta t_c/\Delta t_b$ (sec)	Coloration efficiency (cm^2/C)	Ref.
ITO/WO_3/PVB-based GPEFs/$Ni_{1-x}O$/ITO	4.0×10^{-5} at room temperature	65.8 (550 nm)	16.5/9.5	175.34	20
ITO/WO_3/ED2003-GLYMO-CA/ITO	1.6×10^{-4} at 30℃	35 (550 nm)	17/28	183	29
FTO/WO_3/PMMA-[Emim]BF4 composite electrolyte/FTO	2.9×10^{-3} at room temperature	71 (632.8 nm)	62.6/41.2	55.3	30
ITO/WO_3/PVDF-co-HFP-based gel electrolyte with dmFc/ITO	6.7×10^{-3} at 20℃	84.8 (700 nm)	14/24	58.2	31
ITO/WO_3/PMMA-based gel electrolyte with Fc/ITO/	6.81×10^{-5} at room temperature	81.92 (700 nm)	9/17	95.44	This work

area (121 cm^2) ECD was successfully fabricated using bar-coated WO_3 and the PMMA-based GPE by employing the lamination process. Because the bar-coating process of WO_3 can be applied as a roll-to-roll process, it is expected to be very suitable for the mass production of devices when used in conjunction with the lamination process.

4. CONCLUSION

Flexible ECDs were optimized and successfully fabricated using a PMMA-based GPE with varying concentrations of Fc and hardening times. The electrochromic response of the fabricated ECD was found to vary according to the concentrations of PMMA and Fc and hardening times that were applied before the lamination process. These optimized ECDs were uniformly bonded to each electrode using the PMMA-based GPE with Fc via the lamination process. Therefore, the ECDs were found to exhibit extremely high transmittance changes (ΔT = ~81.92%), high CE (η = 95.44 cm^2/C), and stable performance for repeated bending and electrochromic cycles (4.6% degradation for 10,000 cycles) compared with the values reported in previous studies on ITO/PET substrates. Additionally, a large-area, flexible ECD (121 cm^2) was successfully fabricated using bar-coated WO_3. Hence, the successful fabrication of ECDs employing PMMA-based GPEs with Fc via the lamination process was found to demonstrate that mass production of flexible ECDs is potentially possible when used in conjunction with the roll-to-roll process.

ORCID

Haekyoung Kim https://orcid.org/0000-0002-9870-3905

ACKNOWLEDGEMENTS

This work was supported by the Korea Innovation Foundation (INNOPOLIS) [2020-DD UP-0278] and the National Research Foundation of Korea (NRF) grant funded by the Korea government (MSIT) [NRF- 2022R1A2C100 5585].

REFERENCES

[1] P. V. Rathod, J. M. Puguan, and H. Kim, *Chem. Eng. J.*, **422**, 130065 (2021). [DOI: https://doi.org/10.1016/j.cej.2021.130065]

[2] S. Nundy, A. Mesloub, B. M. Alsolami, and A. Ghosh, *J. Clean. Prod.*, **301**, 126854 (2021). [DOI: https://doi.org/10.1016/j.jclepro.2021.126854]

[3] A. Abdollahi, H. R. Mamaqani, and B. Razavi, *Prog. Polym. Sci.*, **98**, 101149 (2019). [DOI: https://doi.org/10.1016/j.progpolymsci.2019.101149]

[4] C. Sella, M. Maaza, O. Nemraoui, J. Lafait, N. Renard, and Y. Sampeur, *Surf. Coat. Technol.*, **98**, 1477 (1998). [DOI: https://doi.org/10.1016/S0257-8972(97)00154-0]

[5] Y. Ke, J. Chen, G. Lin, S. Wang, Y. Zhou, J. Yin, P. S. Lee, and Y. Long, *Adv. Energy Mater.*, **9**, 1902066 (2019). [DOI: https://doi.org/10.1002/aenm.201902066]

[6] S. Lin, X. Bai, H. Wang, H. Wang, J. Song, K. Huang, C. Wang, N. Wang, B. Li, M. Lei, and H. Wu, *Adv. Mater.*, **29**, 1703238 (2017). [DOI: https://doi.org/10.1002/adma.201703238]

[7] L. M. Huang, C. W. Hu, H. C. Liu, C. Y. Hsu, C. H. Chen, and

K. C. Ho, *Sol. Energy Mater. Sol. Cells*, **99**, 154 (2012). [DOI: https://doi.org/10.1016/j.solmat.2011.03.036]

[8] P. Yang, P. Sun, and W. Mai, *Mater. Today*, **19**, 394 (2016). [DOI: https://doi.org/10.1016/j.mattod.2015.11.007]

[9] A. Subrahmanyam, C. S. Kumar, and K. M. Karuppasamy, *Sol. Energy Mater. Sol. Cells*, **91**, 62 (2007). [DOI: https://doi.org/10.1016/j.solmat.2006.07.003]

[10] Y. Ding, M. A. Invernale, D.M.D. Mamangun, A. Kumar, and G. A. Sotzing, *J. Mater. Chem*., **21**, 11873 (2011). [DOI: https://doi.org/10.1039/C1JM11141H]

[11] W. Li, T. Bai, G. Fu, Q. Zhang, J. Liu, H. Wang, Y. Sun, and H. Yan, *Sol. Energy Mater. Sol. Cells*, **240**, 111709 (2022). [DOI: https://doi.org/10.1016/j.solmat.2022.111709]

[12] Z. Jiao, X. W. Sun, J. Wang, L. Ke, and H. V. Demir, *J. Phys. D: Appl. Phys.*, **43**, 285501 (2010). [DOI: https://doi.org/10.1088/0022-3727/43/28/285501]

[13] V. K. Thakur, G. Ding, J. Ma, P. S. Lee, and X. Lu, *Adv. Mater*., **24**, 4071 (2012). [DOI: https://doi.org/10.1002/adma.201200213]

[14] F. Baskoro, H. Q. Wong, and H. J. Yen, *ACS Appl. Energy Mater*., **2**, 3937 (2019). [DOI: https://doi.org/10.1021/acsaem.9b00295]

[15] W. Li, Y. Pang, J. Liu, G. Liu, Y. Wang, and Y. Xia, *RSC Adv*., **7**, 23494 (2017). [DOI: https://doi.org/10.1039/C7RA02603J]

[16] H. Gao, W. Zhou, K. Park, and J. B. Goodenough, *Adv. Energy Mater*., **6**, 1600467 (2016). [DOI: https://doi.org/10.1002/aenm.201600467]

[17] R. Zhang, Y. Chen, and R. Montazami, *Materials*, **8**, 2735 (2015). [DOI: https://doi.org/10.3390/ma8052735]

[18] F. Bella, A. Lamberti, S. Bianco, E. Tresso, C. Gerbaldi, and C. F. Pirri, *Adv. Mater. Technol*., **1**, 1600002 (2016). [DOI: https://doi.org/10.1002/admt.201600002]

[19] S. Desai, R. L. Shepherd, P. C. Innis, P. Murphy, C. Hall, R. Fabretto, and G. G. Wallace, *Electrochim. Acta*, **56**, 4408 (2011). [DOI: https://doi.org/10.1016/j.electacta.2010.10.030]

[20] F. Zhang, G. Dong, J. Liu, S. Ye, and X. Diao, *Ionics*, **23**, 1879 (2017). [DOI: https://doi.org/10.1007/s11581-017-1996-y]

[21] J.M.C. Puguan, W. J. Chung, and H. Kim, *Electrochim. Acta*, **196**, 236 (2016). [DOI: https://doi.org/10.1016/j.electacta.2016.02.172]

[22] J. Bae, H. Kim, H. C. Moon, and S. H. Kim, *J. Mater. Chem. C*, **4**, 10887 (2016). [DOI: https://doi.org/10.1039/C6TC03463B]

[23] K. Ahmad, M. A. Shinde, G. Song, and H. Kim, *Ceram. Int*., **47**, 34297 (2021). [DOI: https://doi.org/10.1016/j.ceramint.2021.08.340]

[24] J. Bae, D. G. Seo, S. M. Park, K. T. Park, H. Kim, H. C. Moon, and S. H. Kim, *J. Phys. D: Appl. Phys.*, **50**, 465105 (2017). [DOI: https://doi.org/10.1088/1361-6463/aa8e88]

[25] J. Y. Wang, M. C. Wang, and D. J. Jan, *Sol. Energy Mater. Sol. Cells*, **160**, 476 (2017). [DOI: https://doi.org/10.1016/j.solmat.2016.11.009]

[26] D. Saikia, C. C. Han, and Y.W.C. Yang, *J. Power Sources*, **185**, 570 (2008). [DOI: https://doi.org/10.1016/j.jpowsour.2008.06.063]

[27] S. N. Asmara, M. Z. Kufian, S. R. Majid, and A. K. Arof, *Electrochim. Acta*, **57**, 91 (2011). [DOI: https://doi.org/10.1016/j.electacta.2011.06.045]

[28] S. Chandra, S. S. Sekhon, and N. Arora, *Ionics*, **6**, 112 (2000). [DOI: https://doi.org/10.1007/BF02375554]

[29] D. Saikia, C. G. Wu, J. Fang, L. D. Tsai, and H. M. Kao, *J. Power Sources*, **269**, 651 (2014). [DOI: https://doi.org/10.1016/j.jpowsour.2014.06.159]

[30] Q. Tang, H. Li, Y. Yue, Q. Zhang, H. Wang, Y. Li, and P. Chen, *Mater. Des*., **118**, 279 (2017). [DOI: https://doi.org/10.1016/j.matdes.2017.01.033]

[31] T. Y. Yun, X. Li, J. Bae, S. H. Kim, and H. C. Moon, *Mater. Des*., **162**, 45 (2019). [DOI: https://doi.org/10.1016/j.matdes.2018.11.016]

[32] G. Y. Karaca, E. Eren, G. C. Cogal, E. Uygun, L. Oksuz, and A. U. Oksuz, *Opt. Mater*., **88**, 472 (2019). [DOI: https://doi.org/10.1016/j.optmat.2018.11.052]

[33] H. W. Choi, D. G. Seong, and J. S. Park, *Org. Electron*., **87**, 105970 (2020). [DOI: https://doi.org/10.1016/j.orgel.2020.105970]

[34] Y. Wang, Z. Meng, H. Chen, T. Li, D. Zheng, Q. Xu, H. Wang, X. Y. Liu, and W. Guo, *J. Mater. Chem. C*, **7**, 1966 (2019). [DOI: https://doi.org/10.1039/C8TC05698F]

[35] X. Liu, K. Li, C. Hou, H. Li, P. Chen, Q. Zhang, Y. Li, and H. Wang, *Mater. Sci. Eng.: B*, **241**, 36 (2019). [DOI: https://doi.org/10.1016/j.mseb.2019.02.001]

[36] Y. Kim, C. Park, S. Im, and J. H. Kim, *Sci. Rep*., **10**, 16488 (2020). [DOI: https://doi.org/10.1038/s41598-020-73259-x]

[37] E. Eren, C. Alver, G. Y. Karaca, E. Uygun, L. Oksuz, and A. U. Oksuz, *Electroanal*., **30**, 2099 (2018). [DOI: https://doi.org/10.1002/elan.201800276]

[38] M. Wang, A. Barnabé, Y. Thimont, J. Wang, Y. He, Q. Liu, X. Zhong, G. Dong, J. Yang, and X. Diao, *Electrochim. Acta*, **301**, 200 (2019). [DOI: https://doi.org/10.1016/j.electacta.2019.01.184]